Antiviral Research 87 (2010) 345–352

Contents lists available at ScienceDirect

Antiviral Research

journal homepage: www.elsevier.com/locate/antiviral

High yield synthesis, purification and characterisation of the RNase L activators 5′-triphosphate 2′–5′-oligoadenylates

B. Morin [a], N. Rabah [a], J. Boretto-Soler [a], H. Tolou [b], K. Alvarez [a,*], B. Canard [a,*]

[a] Architecture et Fonction des Macromolécules Biologiques, CNRS and Universités d'Aix-Marseille I et II, UMR 6098, ESIL Case 925, 13288 Marseille, France
[b] Unité de Virologie Tropicale, IMTSSA, BP 46, 13998, Marseille Armées, France

ARTICLE INFO

Article history:
Received 7 April 2010
Received in revised form 1 June 2010
Accepted 7 June 2010

Keywords:
Antiviral
2′–5′ Oligoadenylate
Oligoadenylate synthetase
Ribonuclease L
HPLC

ABSTRACT

Upon viral infection, double-stranded viral RNA is detected very early in the host cell by several cellular 2′–5′ oligoadenylate synthetases, which synthesize 2′–5′ adenylate oligonucleotides that activate the cellular RNase L, firing an early primary antiviral response through self and non-self RNA cleavage. Transfecting cells with synthetic 2′–5′ adenylate oligonucleotides activate RNase L, and thus provide a useful shortcut to study the early steps of cellular and viral commitments into this pathway. Defined 2′–5′ adenylate oligonucleotides can be produced *in vitro*, but their controlled synthesis, purification, and characterisation have not been reported in detail. Here, we report a method suitable to produce large amounts of 2–5As of defined lengths *in vitro* using porcine OAS1 (pOAS) and human OAS2 (hOAS). We have synthesized a broad spectrum of 2–5As at the milligram scale and report an HPLC-purification and characterisation protocol with quantified yield for 2–5A of various lengths.

1. Introduction

The mammalian cell response to a viral infection is mainly mediated by type I interferon-regulated pathways (Sen, 2001; Servant et al., 2002). One of the main and early effects is to activate the 2′–5′ oligoadenylate synthetase (OAS)/ribonuclease L (RNase L) pathway (Roberts et al., 1976), where double-stranded non-self RNA produced during infection by the viral invader is recognized by one or several OAS isoforms. This enzyme is allosterically activated by dsRNA to synthesize small specific RNA molecules which are oligomers of adenosine with the particularity to be linked by 2′–5′ phosphodiester bonds instead of 3′–5′ as in "classic" RNAs (Hovanessian and Justesen, 2007). These oligomers (2–5As) are known to bind RNase L (Dong and Silverman, 1995), and the 2′–5′ phosphodiester bonds have been shown to be essential for the specific binding. The structural basis of this activation has been reported in the crystallographic structure of the 2–5A:RNase L complex (Tanaka et al., 2004), currently the only example of protein crystallized in complex with 2–5As. Once activated, RNase L cleaves both cellular and viral single-stranded RNA, thus playing an important role in the endogenous antiviral pathway (Silverman, 2007b). In recent years, several correlations between viral infections and the OAS/RNase L pathway have been reported (Behera et al., 2002; Kajaste-Rudnitski et al., 2006; Sawicki et al., 2003; Smith et al., 2005). Conversely, the ability of some viruses to counteract the antiviral action of RNase L has also been demonstrated (Han et al., 2007; Min and Krug, 2006; Xiang et al., 2002). Precise mechanisms remain ill-defined, though, and mechanisms of indirect or direct interaction between viral proteins and the OAS/RNase L pathway remain to be discovered.

No direct interaction of a viral protein with 2–5As has been reported yet. Conceptually, however, these 2–5As represent early triggers of the non-specific innate immune response, and thus, early viral interference with this pathway would be expected to efficiently dampen the host response to viral invasion. Indeed, direct induction of the RNase L response with these purified oligomers has been achieved successfully through transfection of 2–5A (Malathi et al., 2007; Silverman, 2007a). Likewise, activation of RNase L by small organic molecules has been shown to efficiently launch an antiviral state in the host cell (Thakur et al., 2007). Thus, it would be logic that viruses had evolved a way to interfere early with the innate immune response which involves the induction of more than a thousand actors in a potent and complex antiviral response.

With this idea in mind, we set up to obtain high amounts of pure and structurally characterised 2–5A in order to study their interaction with potential viral targets before they reach RNase L in the cell cytoplasm.

Several 2–5A synthesis protocols have been described, using either chemical or enzymatic method (Imai and Torrence, 1981;

Abbreviations: DP, degree of polymerisation; OAS, oligoadenylate synthetase; pOAS1, porcine OAS 1; hOAS2, human OAS 2; 2–5A, 2′–5′ oligoadenylate; RNase L, ribonuclease L; CIP, calf alkaline phosphatase; VCE, vaccinia virus capping enzyme; RNase T2, ribonuclease T2.

* Corresponding authors. Tel.: +33 4 91 82 86 44; fax: +33 4 91 82 86 46.
E-mail addresses: karine.alvarez@afmb.univ-mrs.fr (K. Alvarez), bruno.canard@afmb.univ-mrs.fr (B. Canard).

0166-3542/$ – see front matter © 2010 Elsevier B.V. All rights reserved.
doi:10.1016/j.antiviral.2010.06.003

Justesen et al., 1980; Kitade et al., 1991; Rusch et al., 2001; Thakur et al., 2007). However, the chemical synthesis of a 5′-triphosphate, a *sine qua non* condition to retain RNase L activation, is not easy and has been reported in an eight-step synthesis. In addition, neither easy nor large-scale production nor detailed purification, reporting yield, size distribution, and individual fractionation of size-controlled 2–5A, has been documented.

The enzymatic synthesis of 2–5A has been reported using purified OASs. Human OASs belong to a family of enzymes encoded by 3 closely linked genes with the following order: small (OAS1), medium (OAS2) and large (OAS3) isoforms, corresponding to proteins of 40/46, 69/71 and 100 kDa respectively. They are composed of one, two or three repeats of the basic OAS module, corresponding to their size (Hovanessian and Justesen, 2007). At their optimum activity conditions, OAS1 and OAS2 have the capacity to synthesize oligomers of "high" molecular weight, whereas OAS3 has the tendency to synthesize preferentially dimeric oligonucleotides. Some of these enzymes have been used to synthesize 2–5As (Rebouillat and Hovanessian, 1999), but no detailed protocol, precise purification, nor characterisation of the synthesized products has been described.

Here we report a protocol to produce large amount of different 2–5As *in vitro*. Two OASs, the porcine OAS1 (pOAS1) and the human OAS2 (hOAS2), were used and compared to synthesize a broad spectrum of 2–5As at the milligram scale with quantified yield for 2–5A of various lengths. We show that the Vaccinia virus mRNA capping enzyme is active as an RNA 5′-triphosphatase on the 2–5As, providing a simple and robust method to prepare 2–5A with a 5′-diphosphate. The purified 2–5As are able to induce rRNA degradation in transfected cell, as expected for an RNase L-mediated antiviral response.

2. Materials and methods

2.1. Expression and purification of recombinant human OAS2 in insect cells

The human OAS2 cDNA cloned in pFastBac vector (Invitrogen Bac-to-Bac Baculovirus Expression System) as a N-terminal His-tag fusion protein was a kind gift of Saumendra N. Sarkar and Games C. Sen from The Lerner Research Institute, Cleveland, USA. This construction was transformed into DH10-Bac *Escherichia coli* to produce bacmid DNA. The presence of recombinant bacmids was verified by PCR, and bacmids were used for the generation of human OAS2 recombinant baculovirus using Invitrogen Bac-to-Bac Baculovirus Expression System. All experiments were carried out according to the manufacturer's protocol in insect Sf9 cells. Sf9 insect cells were maintained in a spinner or monolayer cultures at 27 °C in Insect-XPress medium (BioWhittaker, Lonza). For large-scale production of the hOAS2 isoenzyme, 3×10^8 Sf9 cells were infected. 72 h post-infection, cells were harvested and the hOAS2 protein was purified as described in Sarkar and Sen (1998).

2.2. Expression and purification of recombinant porcine OAS1 in E. coli

The optimized gene of porcine OAS1 cloned into pET-15b as an N-terminal His-tag fusion protein was purchased from Geneart (Germany). The protein was expressed in BL21 (DE3) p*LysS* (Stratagene, U.S.A.) at 25 °C overnight after induction with 0.5 mM IPTG in LB Broth. The protein was purified in two steps, first with cation exchange chromatography (Cellulose Phosphate P11, Whatman) in 50 mM $NaPO_4$ buffer pH 7.5, 10% glycerol, 1 mM DTT, 0.1% Igepal CA630 (Sigma–Aldrich), 1 mM EDTA, and 50 mM NaCl. A gradient from 50 mM to 0.5 M NaCl was applied, and the protein was eluted at 0.32 M NaCl. Fractions were collected and applied to an immobilized metal affinity chromatography column (Ni-NTA, GE Healthcare) in 50 mM $NaPO_4$ buffer pH 7.5, 45 mM imidazole, 10% glycerol, 0.1% Igepal CA630, 1 mM EDTA, and 0.32 M NaCl. After washing with the same buffer, the protein was eluted in the same buffer supplemented with 240 mM imidazole (final concentration). The collected protein was dialysed against the same buffer without imidazole. The last dialysis buffer change constituted the storage buffer, i.e., 50 mM $NaPO_4$ pH 7.5, 50% glycerol, 0.3 M NaCl, 0.5 mM EDTA and 5 mM β-mercaptoethanol.

2.3. HPLC set-up

A Waters model 600 gradient HPLC system equipped with two 600 pumps, a 717 plus Autosampler injector, and a 996 photodiode array detector. An in-line degasser AF was employed for reverse phase chromatography. The separation column (Reverse Phase C18) and a pre-column (Reverse Phase C18) were installed in parallel on a two 7000 Rheodyne valve system (Interchim) for the online-cleaning procedure. A filter insert protected the column assembly. As buffer stock solution a 1 M solution of triethylammonium bicarbonate (TEAB) was prepared by adding dry-ice to a 1 M triethylamine solution until the pH reached 7.4 and filtered through 0.22 μM GV-type membranes (Millipore). HPLC eluents were freshly prepared. Eluent A was a 0.05 M solution of TEAB (pH 7.4) and eluent B was a 1:1 mixture of acetonitrile (HPLC grade, SDS, Peypin, France) and TEAB (final concentration 0.05 M, pH 7.4). The applied gradients for analytical and preparative separation of 2–5As are described in the corresponding sections (see below).

For HPLC coupled mass spectrometry, a Waters model Alliance 2790 system equipped with a photodiode array detector was employed. Mass spectra were recorded on an analyzer Quadrupole time-of-flight "Qtof" mass spectrometer (Waters). Conditions were accelerating potential 20 V, capillary potential 3000 V, source temperature 150 °C and nebulization temperature 250 °C.

2.3.1. Analytical scale

20 μl of sample was mixed with 180 μl of TEAB (0.05 M) and analysed. The column assembly consists of a pre-column (Delta-pak C18 100 Å, 5 μm, 3.9 × 20 mm) and a separation column (Nova-pak C18, 4 μm, 3.9 × 150 mm). Separations were run at a flow rate of 1 ml/min and started with a 5 min elution (100% eluent A) on the pre-column to remove proteic material. The analytical gradient started after 5 min at 100% eluent A with an increase to 8% eluent B after 15 min, to 15% eluent B after 30 min, to 20% eluent B after 35 min and to 100% eluent B after 40 min.

2.3.2. Preparative scale

250 μl of sample was mixed with 400 μl of TEAB (0.05 M) and analysed. The column assembly consists of a pre-column (XTerra prep MSC18, 10 μm, 10 × 10 mm) and a separation column (XTerra prep MSC18, 10 μm, 10 × 250 mm). Separations were run at a flow rate of 5 ml/min and started with a 5 min elution (100% eluent A) on the pre-column to remove proteic material. The analytical gradient started after 5 min at 100% eluent A with an increase to 8% eluent B after 15 min, to 15% eluent B after 30 min, to 20% eluent B after 35 min and to 100% eluent B after 40 min.

2.4. Mass spectrometry analysis

MALDI-TOF mass spectra were recorded on a Voyager DE mass spectrometer (Perseptive Biosystems, Framingham, MA, USA) equipped with an N_2 laser (337 nm). MALDI conditions were accelerating potential, 24,000 V; guide wire, 0.05% of accelerating voltage; grid voltage, 94% of accelerating voltage; delay extraction time, 550 ns. Spectra were obtained in negative mode and were

not smoothed. The oligonucleotides (100 pmol) were suspended in 10 μl of water and desalted using drop dialysis through a membrane filter WSWP 0.025 μm, 13 mm (Millipore) floating on a 0.1 M ammonium citrate solution for 30 min. When drop dialysis did not allow the removal of all salt traces, the samples were further treated with a few beads of DOWEX 50W X8 resin (ammonium form) before spotting them on the MALDI target. Samples of 0.5 μl were mixed with 0.5 μl of the matrix 2,4,6-trihydroxyacetophenone (THAP, 45 mg, ammonium citrate, 4 mg in 500 μl acetonitrile/water, 1:1, v/v) and the mixtures were spotted on the stainless steel MALDI target and left to dry under air before MALDI analysis.

2.5. HPLC coupled mass spectrometry

Samples were previously filtered on Microcon (size exclusion >3000 Da) (Millipore) to remove proteic material. 20 μl of sample was mixed with 20 μl of TEAB (0.05 M) and analysed. The column assembly consists of a pre-column (Delta-pak C18 100 Å, 5 μm, 3.9 × 20 mm) and a separation column (Nova-pak C18, 4 μm, 3.9 × 150 mm). Separations were run at a flow rate of 1 ml/min. The analytical gradient started after 5 min at 100% eluent A with an increase to 8% eluent B after 15 min, to 15% eluent B after 30 min, to 20% eluent B after 35 min and to 100% eluent B after 40 min. The flow was split in tandem UV and MS. Mass spectra were obtained in negative mode (electrospray ion source).

2.6. 2–5A synthetase activity assay

The 2–5A synthetase activity assay was performed by incubating the recombinant protein (2 μM of pOAS1 or 1 μM of hOAS2) in a reaction mixture containing 20 mM Tris/base pH 7.5, 20 mM $MgCl_2$, 2.5 mM DTT, 50 μg/ml poly (I:C), 10 mM ATP as a substrate in a final volume of 50 μl at 30 °C. The reaction was stopped by heating at 95 °C for 5 min and analysed on HPLC. In the case of radiolabel-containing reactions, 0.4 μCi/μl of (γ-^{32}P) ATP was added to the mixture. The reaction was stopped by the addition of a standard gel-loading formamide Blue Dye/EDTA solution and heating at 95 °C for 5 min. The 2–5A products were then analysed by electrophoresis on 14% polyacrylamide gels containing 7% urea in TTE buffer (89 mM Tris–HCl, pH 8.0, 28 mM taurine, 0.5 mM EDTA). For reactions using 2 substrates, 7 mM of ATP and 3 mM of the other (ADP or AMP) was added to the mixture, and incubated for 2 h.

2.7. Large-scale synthesis of triphosphate 2–5A

A preparative reaction (1 ml) was set up using the same conditions as described above, with 2 μM of pOAS1 for 2 h, and samples of 250 μl reaction mixture were injected into the HPLC system. The different peaks were collected, and fractions corresponding to each oligomer were pooled together. Finally, the pooled fractions were lyophilised two times and the concentration was determined. The ε_{260} values (M^{-1} cm^{-1}) of 2–5As used were 30,800, 46,200, 61,600, 77,000 and 92,400 for the dimer, trimer, tetramer, pentamer and hexamer respectively.

2.8. Vaccinia virus 5′-RNA triphosphatase activity

25 μl of the synthetase reaction mixture was treated with 80 units of Vaccinia virus capping enzyme (Epicentre Biotechnologies) at 37 °C for 2 h. The reaction was stopped by heating at 95 °C for 5 min and analysed by HPLC.

2.9. CIP alkaline phosphatase activity

100 μl of the synthetase reaction mixture was treated with 10 units of Calf alkaline phosphatase (CIP) (Biolabs) at 25 °C for 1 h. The reaction was stopped by heating at 95 °C for 5 min and analysed by HPLC.

2.10. RNase T2 phosphodiesterase activity

After reaction, purification, separation and collection (using large-scale conditions), the sample corresponding to the 5′-triphosphate trimer was lyophilised two times and re-suspended in water. The purity was verified by HPLC, its concentration determined by measuring OD_{260} values and the molecular mass was verified by mass spectrometry (MALDI-TOF). 50 nmols of 2–5A trimer was then treated with 1 unit of CIP and injected into the HPLC system for purification (using large-scale conditions). The peak corresponding to the 5′-hydroxyl 2–5A trimer was collected, lyophilised two times and re-suspended in water. 20 nmols of the 2–5A and 3–5A (Dharmacon) trimer having 5′-hydroxyl ends were treated with 23 units of RNase T2 (Gibco BRL) at 37 °C for 1 h. The reaction was stopped by heating at 95 °C for 5 min, loaded onto the HPLC column and analysed by mass spectrometry.

2.11. Cell transfections and RNAse L-mediated rRNA cleavage

Hela cells (human cervical epithelial cells) were grown in DMEM supplemented with 10% heat-inactivated fetal bovine serum (Biotech GmBH) and streptomycin–penicillin (Gibco). Cells were plated 1 day before transfection in order to be 50–60% confluent by the time of transfection. 2–5As were transfected using Oligofectamine Reagent (Invitrogen) according to the manufacturer's protocol. Cells were harvested 3 h after transfection and washed with ice cold PBS. Total RNA was extracted from transfected cells using Qiagen RNeasy isolation kit (Qiagen) according to the manufacturer's instructions. rRNA degradation was analysed using agarose gel electrophoresis. RNA samples (2 μg) were heat-denatured 10 min at 70 °C in RNA loading buffer (50% formamide, 6% formaldehyde and 5% glycerol in MOPS buffer), then separated on 1% agarose gel in MOPS buffer.

3. Results and discussion

3.1. Kinetics and product distribution during hOAS2- and pOAS1-mediated synthesis of 2–5A oligomers

In order to cover a wide degree of polymerisation (DP) of 2–5A products, we chose the porcine OAS1 (pOAS1) and the human OAS2 (hOAS2) oligoadenylate synthetase as catalysts in enzymatic reaction synthesizing 2–5As from ATP. An OAS3 enzyme was not included in the study since such protein catalyses mainly the production of 2′–5′ dimers (Rebouillat et al., 1999). The enzymes were expressed and purified from recombinant cloned genes in *E. coli* and insect cells for pOAS1 and hOAS2 (Hartmann et al., 2003; Kodym et al., 2009; Sarkar and Sen, 1998), respectively (see Section 2). We obtained ~450 μg of purified hOAS2 and 60 mg of purified pOAS1 per liter of culture, both with a ~90% purity as judged by denaturing PAGE. For enzyme characterisation, we tested published experimental conditions for these proteins (Marie et al., 1997; Sarkar and Sen, 1998), except that a high concentration of substrate (ATP 10 mM) was used in an attempt to maximize the overall yield. However, at concentrations above 10 mM, substrate inhibition became prevalent (data not shown). We first selected the lowest concentration of each protein giving a wide range of oligomer products, as detected in PAGE separated products containing (γ-^{32}P) AMP in 5′ (i.e., using (γ-^{32}P) ATP as a substrate, Fig. 1). The radiolabel incorporated in each band product was counted in the region of the gel corresponding to each of the 2–5A oligomers, and plotted in a graph (Fig. 1).

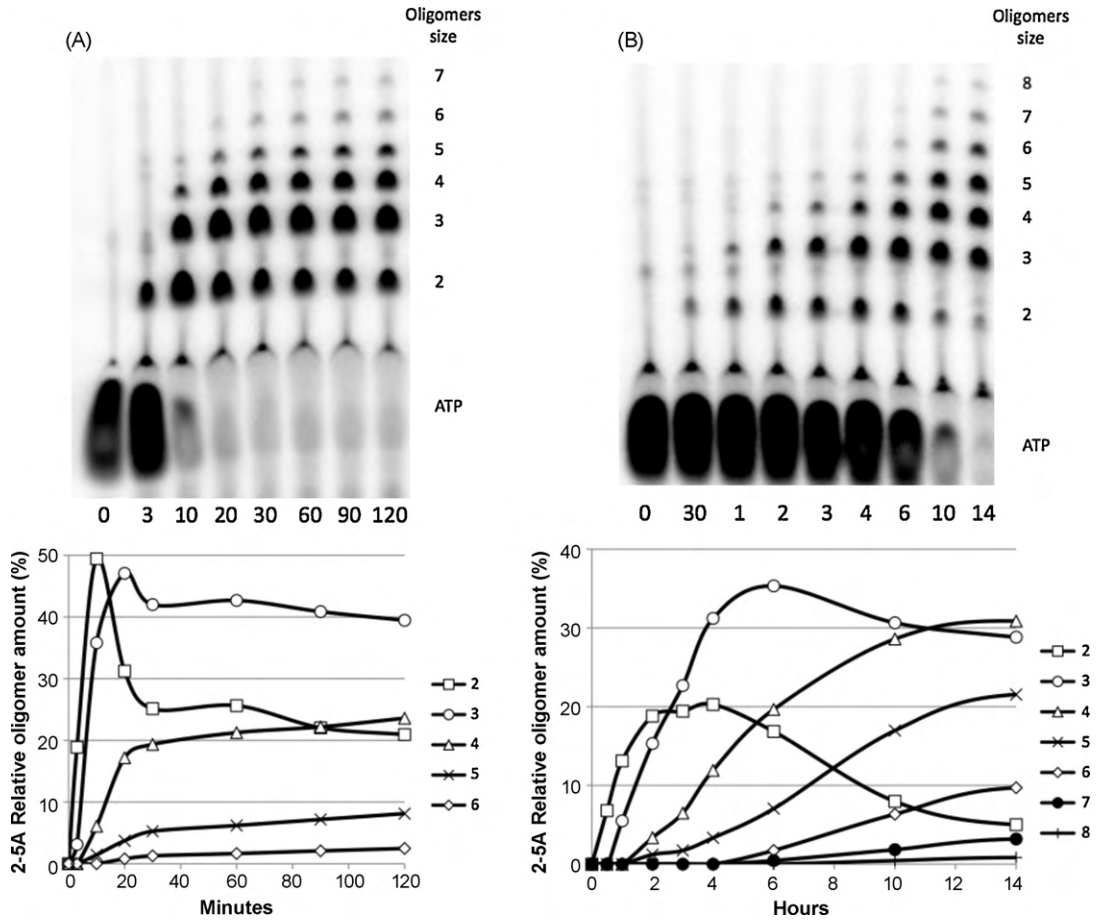

Fig. 1. Time course reaction of 2–5A synthesis. The OAS activity of both the porcine (A) and human (B) OAS was assayed using (γ-^{32}P) ATP. Reaction conditions were as described in Section 2. The reaction was stopped at different times and the 2–5A products were analysed by PAGE, and the gel was auto-radiographed. The radioactivity of the spots corresponding to each oligomer was counted and the values were expressed as a percentage of total products formed at the end of the reaction. The values are shown in the graphic below the corresponding autoradiogram. □: dimer, ○: trimer, △: tetramer, ×: pentamer, ◊: hexamer, ●: heptamer, and |: octamer.

As expected from enzymes from type 1 and type 2 families, the size distribution of the products is well over the dimer. The product DP varies between these two polymerases, in accordance with the reported difference in processivity (Hovanessian and Justesen, 2007). The reaction reaches equilibrium much faster in pOAS1 (1 h) (Fig. 1A) than in hOAS2 (>12 h) (Fig. 1B). A clear preference for the trimer is observed for both at equilibrium, although pOAS1 synthesizes before equilibrium (after 10 min) a maximum of dimer in absolute. However, the pOAS1 is less stable and precipitates during the reaction in contrast to the hOAS2 which does not. We did not investigate on this observation further, although it should prove helpful if the dimer synthesis yield is to be optimized. In the case of pOAS1 (Fig. 1A), the trimer is the major oligomer in the mixture at equilibrium and represents 40% of the total products, while dimer and tetramer represent around 22% of the total products formed. Longer oligomers represent less than 10%, which renders their production more problematic.

In the case of the hOAS2, the reaction is much slower than but similar to that of pOAS1 in the early stage (Fig. 1B). After 14 h of reaction, the size distribution of the products formed during the reaction is stable and in contrast to pOAS1, a very low concentration of dimer remains, as if it had been used in the reaction and converted to products of higher DP. The final proportions of trimer and tetramer are around 30% of total products, followed by the pentamer (22%) and hexamer (10%). At the end of the reaction, the amount of pentamer produced using hOAS2 is close to that of tetramer produced using pOAS1. Overall, the OASs are polymerases of low processivity compared to e.g., RNA polymerases, allowing appropriate control of product size.

3.2. Production of 5′ triphosphate, 5′ diphosphate and 5′ hydroxyl 2–5A

In order to produce 2–5A oligomers with various 5′-ends, the synthesized reaction products were treated with phosphatase to generate two different types of 5-ends: a 5′-diphosphate and 5′-hydroxyl. The commercial Vaccinia Virus capping enzyme (VCE) is known to possess all the activities essential for RNA capping which are the triphosphatase, the guanyltransferase and the methyltransferase (Shuman, 1990). In our experiment, the triphosphatase activity was used in order to generate oligomers with a 5′-diphosphate end. Calf intestine phosphatase (CIP), known to remove all 5′-phosphates (Kim and Wyckoff, 1991) was also used to generate 5′-hydroxyl RNAs. First, a 2–5A synthesis reaction was performed as described in Section 2, with 2 μM of pOAS1 during 15 min. The reaction was stopped, split in two, and two separate subsequent reactions were performed: one with VCE and the other with CIP. Then, the three reactions were analysed by HPLC. Mass spectrometry analysis was performed in order to identify every peak product (Fig. 2). Hence, analysis of the synthesis reaction on HPLC shows 4 major peaks which correspond respectively to the residual ATP, the dimer, the trimer and the tetramer (Fig. 2, lane 1). Upstream of each of these peaks has small peaks corresponding to each 5′-diphosphate oligomers generated by the formation of ADP during the reaction. After incubation with the VCE (Fig. 2, lane

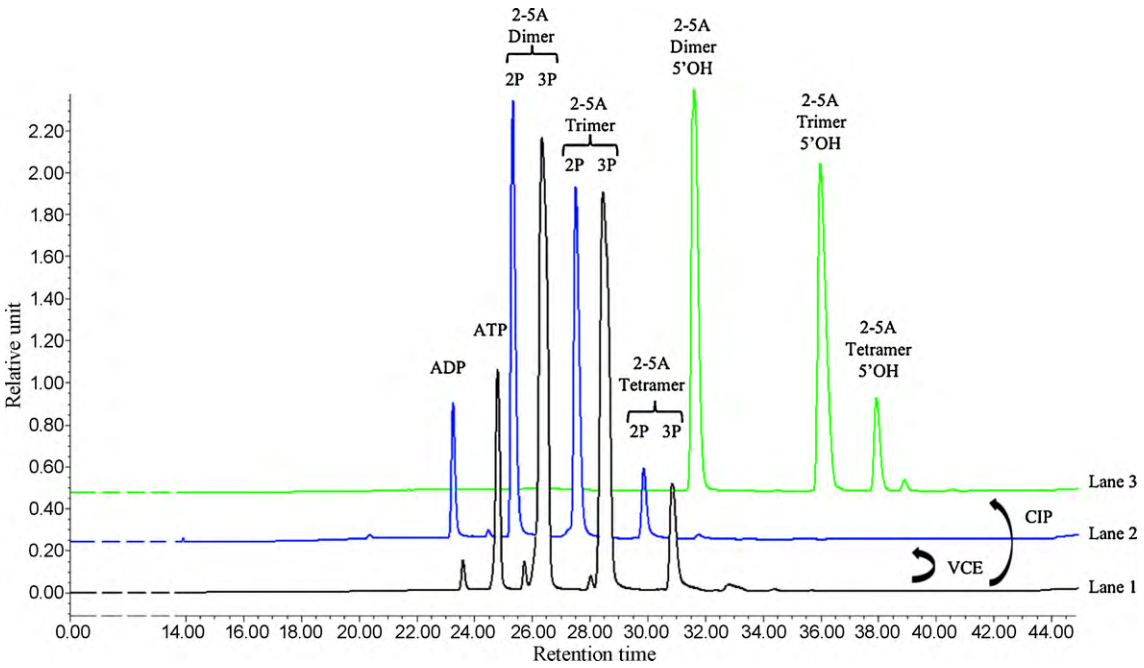

Fig. 2. HPLC profiles of synthesis and phosphatase reaction experiments. A synthesis reaction was performed for 15 min using condition described in Section 2. The reaction mixture was devised in two samples, one load on the HPLC system (lane 1, in black), the second used for phosphatase experiments. Two phosphatase experiments, using VCE (lane 2, in blue) and CIP enzymes (lane 3, in green), were performed to cleave 5′ triphosphatase to generate a diphosphate or a hydroxyl 5′-end, respectively. Reaction conditions are given in Section 2. The reaction products were then loaded on an HPLC system (Delta-pak C18 100 Å, and Nova-pak C18). The gradient started after 5 min at 100% eluent A with an increase to 8% eluent B after 15 min, to 15% eluent B after 30 min, to 20% eluent B after 35 min and to 100% eluent B after 40 min. The corresponding composition of each peak is indicated above them. 5′-Triphosphate ends are labeled 3P, 5′-diphosphate end are labeled 2P, and 5′-hydroxyl ends are labeled 5′-OH. The two arrows indicate the synthetase reaction mixture treated by both VCE and CIP (see Section 2 for details). (For interpretation of the references to colour in this figure legend, the reader is referred to the web version of the article.)

2), we observe a decrease of the retention time for the different major peaks. In fact, the peaks corresponding to the 5′ triphosphate oligomers are transformed into those corresponding to 5′ diphosphate oligomers. Likewise, when the cleavage reaction was performed using CIP (Fig. 2, lane 3), we observed an increase of the retention time of the different products correlated to their size. In contrast to the cleavage with the VCE, the CIP cleaves all the phosphates at the 5′ end of the 2–5A and generates products less charged than the triphosphate 2–5A, which explain the differences observed in retention time. Altogether, these results validate a convenient method of 2–5A oligomer synthesis, either 5′-triphosphate, 5′-diphosphate, or 5′-hydroxyl. We note that it is possible to produce small quantities of 5′-diphosphate and 5′-monophosphate 2–5A, using reaction mixture with two substrates: ATP and ADP, or ATP and AMP (data not shown). The synthesis of 5′-monophosphate 2–5A was not investigated further.

3.3. *Synthesis of triphosphate 2–5A on a preparative scale*

To quantitate the yield of 2–5A oligomer after purification of a 2–5A synthesis, a large-scale 1 ml reaction for 3 h was set up using pOAS1. The entire volume of the reaction was divided into four fractions and injected independently on HPLC. All the peaks corresponding to the triphosphate oligomers were collected and lyophilised two times to remove the volatile buffer solution. Compounds were characterised by mass spectrometry and isolated yields of each oligomer are given in Table 1.

Hence, masses of various oligomers, as measured by mass spectrometry, are in agreement with the theoretical values, namely 835 for the dimer; 1165.76 for the trimer; 1495.30 for the tetramer; 1823.7 for the pentamer; and 2152.05 for the hexamer (Table 1). Based on the mass of recovered products, the best yield (55.5%) was obtained for the trimer. In fact, the amount of trimer recovered after purification is relatively high, close to 1 mg. Yields of two of the other oligomers are also fairly good with a better yield for the tetramer (24.8%) than the dimer (13.9%), and the amount recovered is in the order of several hundreds of μg. At last, but in less proportion, pentamer and hexamer are also recovered during the purification on HPLC. Quantities of product recovered are also significant with more than 80 μg for the pentamer, and more than 10 μg for the hexamer. It is also interesting to note the total amount of product recovered at the end of the purification, which repre-

Table 1
Large-scale synthesis of triphosphate 2–5A oligomers. A preparative reaction was set up with pOAS. For experimental conditions and MALDI-TOF characterisation, see Section 2. Yields are given as isolated values (percentage of formed product, nmol or μg product produced and percentage of ATP conversion) based on absorbance measurements of pure product after lyophilisation. Given retention times correspond to the use of the preparative gradient as described in Section 2.

Size	HPLC retention time (min)	Yields				*m/z* exp. negative mode	*m/z* calc.
		% Formed product	nmol	Mg	%/ATP		
2	23.2	13.9	324.0	269.4	6.5	835.00	836.39
3	25.4	55.5	867.4	1005.8	26	1165.76	1165.59
4	27.5	24.8	289.4	430.6	11.6	1495.30	1494.80
5	29.1	5.1	47.4	86.1	2.4	1823.70	1824.00
5	30.7	0.7	5.2	11.2	0.3	2152.05	2153.21

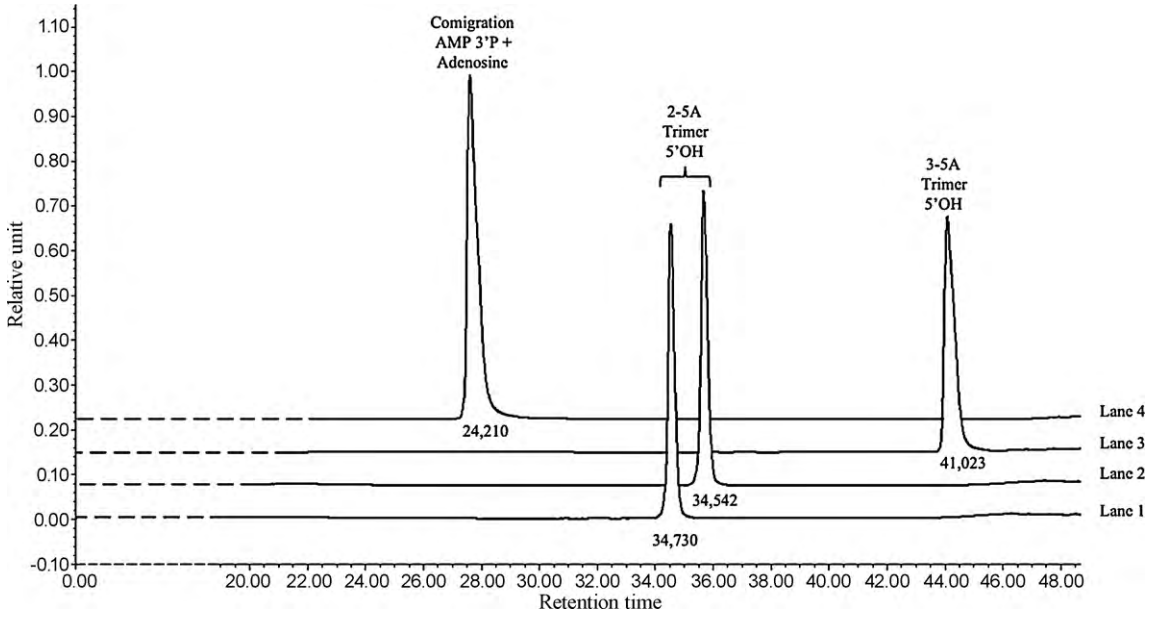

Fig. 3. HPLC profiles of RNase T2 experiments. A preparative reaction was set up and products were purified as described in Section 2. The purified 2–5A trimer fraction was then incubated with the CIP to generate a hydroxyl 5′-end. Commercial 5′-hydroxyl 3–5A trimer (AAA RNA) and the purified 5′-hydroxyl 2–5A trimer were then treated with RNase T2 under conditions described in Section 2. 2–5A trimer (lane 1), 2–5A trimer treated with RNase T2 (lane 2), 3–5A trimer (lane 3) and 3–5A trimer treated with RNase T2 (lane 4) samples, were injected into an HPLC system (Delta-pak C18 100 Å, and Nova-pak C18). The gradient started after 5 min at 100% eluent A with an increase to 8% eluent B after 15 min, to 15% eluent B after 30 min, to 20% eluent B after 35 min and to 100% eluent B after 40 min (see Section 2 for details). The corresponding composition of each peak is indicated above them, and the retention times are indicated under the corresponding peaks.

sents almost 50% of the total ATP used initially for the reaction. This large-scale production of 2–5A oligomers *in vitro* shows that significant amounts of products (mg scale) can be easily recovered after purification of the reaction products by HPLC. It is noteworthy that the HPLC method used here (based on hydrophobic interactions) has the advantage of removing residual salts present in the reaction in contrast to previously reported studies using an ion exchange purification procedure (Budowsky et al., 1994; Xiao et al., 1996).

3.4. Characterisation and structural analysis of 2–5A products

We then set up to characterise the precise structure of 2–5A products in order to design standardized purification protocols. The chemical type of the internucleotidic bonds of the 2–5A products was assayed using phosphodiesterases.

RNase T2 is unable to hydrolyse oligomers having 2′–5′ phosphodiester bonds (Budowsky et al., 1994; Rushizky and Sober, 1963). Two types of trimer were used to assay RNase T2 cleavage: a commercial 3–5A trimer (5′AAA RNA trimer) with a 5′-hydroxyl end, and a 2–5A trimer purified after pOAS1-mediated synthesis. In order to compare trimers, the 2–5A trimer was treated with CIP to release a 5′-hydroxyl end. After the treatment of both 2–5A and 3–5A 5′ hydroxyl-trimers with RNase T2, reactions were analysed using HPLC (Fig. 3). The first characterisation of the difference between 3′–5′ and 2′–5′ phosphodiester bonds is the variation of retention times between the two substrates, ~34 min and ~41 min, respectively (Fig. 3, lane 1 and lane 3). Indeed, the 5′AAA RNA trimer has a retention time increased relative to that of the 2–5A trimer, as described previously (Lesiak et al., 1983). After treatment with the RNase T2, the retention time observed for the entire peak corresponding to the 3–5A trimer was considerably lower (~24 min). Thus, the products of cleavage contained in the peak were characterised by mass spectrometry and two different products were identified: 3′AMP and adenosine. Thus, these two cleavage products had already been identified after the treatment of a 3–5A trimer of adenosine with the RNase T2 (Rushizky and Sober, 1963). As expected, this result shows that the 3–5A trimer is totally degraded by the treatment with the RNase T2. On the contrary, the same experiment made with the 2–5A trimer shows little change in retention time after treatment with RNase T2, indicating that phosphodiester bonds present in the trimer synthesized by the pOAS1 are different from those of the commercial trimer. The variation of retention time between 2–5A and 3–5A trimers and the resistance to the RNase T2 of the 2–5A trimer are both in agreement with the presence of 2′–5′ phosphodiester bonds in oligomers produced by these OASs.

3.5. Analysis of rRNA degradation in transfected cells

Finally, to further characterise the purified 2–5As we tested their effect on the activation of endogenous RNase L in cell transfection experiments. To that end, we transfected Hela cells with increasing concentrations of 2–5A (1–10 μM) and monitored rRNA degradation after 3 h following transfection. As a positive control, synthetic dsRNA poly (I:C), known to induce the OAS/RNase L response (Silverman, 2007b). Poly (I:C) binds to endogenous OASs which activate latent RNase L. The latter cleaves ribosomal RNA thereby leading to 28S and 18S degradation (Fig. 4, and (Silverman, 2007b)). As shown in Fig. 4, the transfection of cells with either oligofectamine alone (mock) or the 2–5A dimer at various concentrations does not induce rRNA degradation since 28S and 18S rRNA bands remain intact. The 2–5A dimer is known to neither bind nor activate RNase L (Xiang et al., 2003). However, the introduction of trimer into cells leads to the appearance of rRNA degradation products (Fig. 4). This degradation is weak at 1 μM and increases with increasing amount of 2–5A. A similar but slightly weaker effect is obtained with tetrameric 2–5A. Functional and structural studies revealed that RNAse L contains three domains namely the N-terminal ankyrin repeat domain, responsible for 2–5A binding, the kinase-like domain and the C-terminal catalytic domain, responsible for catalytic activity (Dong and Silverman, 1997; Nakanishi

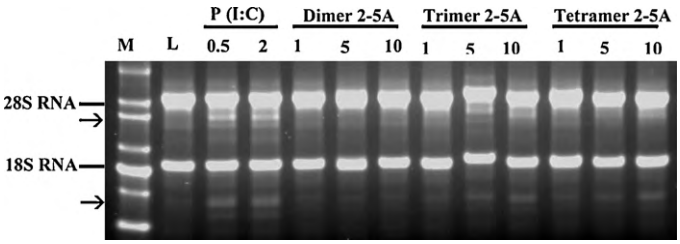

Fig. 4. Analysis of rRNA cleavage in mammalian cells following 2–5A transfection. Hela cells were transfected with oligofectamine reagent alone (Mock), Poly (I:C) at 0.5 and 2 μg/ml or various 2–5As at increasing concentrations (1–10 μM). Total RNA was extracted 3 h after transfection and analysed using agarose gel electrophoresis (see Section 2 for experimental details). M: RNA 0.5–10 kb Ladder; 2 (2–5A): dimer; 3 (2–5A): trimer; 4 (2–5A): tetramer. Arrows indicate rRNA degradation products. Results are representative of three independent experiments.

et al., 2005; Tanaka et al., 2004). The ankyrin domain consists of eight complete ankyrin repeats which will bind the two 2–5A ends (AMP moieties) at repeats 2 and 4. The central AMP moiety is oriented towards the solvent and even if it is involved in weak interactions with the protein it does not interact directly with the ankyrin region (Tanaka et al., 2004), thus pointing out the importance of 2–5A length for RNase L binding and activation (Dong and Silverman, 1997; Nakanishi et al., 2005; Tanaka et al., 2004; Xiang et al., 2003). In fact short 2–5A dimers are not able to interact with both ankyrin repeat sites at the same time and thus are not able to bind nor to activate RNAse L (Tanaka et al., 2004; Xiang et al., 2003). Hence, the physiological effect of the purified 2–5As corresponds to what was previously reported, i.e., the dimer is inactive while the trimer and the tetramer show the expected RNase L activation effect (Tanaka et al., 2004; Xiang et al., 2003).

In conclusion, we have made use of two mammalian OASs to produce a variety of 2–5As that were subsequently HPLC purified and individually characterised. The method described herein is relatively straightforward and does not require a specialized equipment other than an HPLC set-up. The large amount and purity of these 2–5As should prove useful to study the yet ill-defined pathway of viral innate immunity involving 2′5′OAS and RNase L.

Acknowledgments

We wish to thank Jean-Jacques Vasseur (IBMM, Montpellier) for MALDI-TOF spectrometry analysis, Gilles Valette (Plateau technique, Institut des Biomolécules Max Mousseron (IBMM)) for others mass spectrometry analysis, and Saumendra N. Sarkar and Games C. Sen from the Lerner Research Institute, Cleveland, USA for the generous gift of the human OAS2 cDNA clone. The help and advice of Stéphane Canaan and Jean Claude Bakala (IBSM-EIPL, Marseille) in baculovirus expression is gratefully acknowledged. This work was supported by a grant from the Agence Nationale de la Recherche (ANR), programme "Maladies infectieuses et leur environnement", project CHIKVIRULENCE, and a grant from the Direction Générale de l'Armement (contract 09cà40).

Appendix A. Supplementary data

Supplementary data associated with this article can be found, in the online version, at doi:10.1016/j.antiviral.2010.06.003.

References

Behera, A.K., Kumar, M., Lockey, R.F., Mohapatra, S.S., 2002. 2′-5′ Oligoadenylate synthetase plays a critical role in interferon-gamma inhibition of respiratory syncytial virus infection of human epithelial cells. J. Biol. Chem. 277 (28), 25601–25608.

Budowsky, E.I., Kayushina, E.N., Tarasov, A.K., Orlenko, S.A., Cherkasov, I.A., Gavrilov, A.E., Strelenko, Y.A., 1994. Preparation of cyclic 2′,3′-monophosphates of oligoadenylates (A2′p)nA > p and A3′p(A2′p)n-1A > p. Eur. J. Biochem. 220 (1), 97–104.

Dong, B., Silverman, R.H., 1995. 2–5A-dependent RNase molecules dimerize during activation by 2–5A. J. Biol. Chem. 270 (8), 4133–4137.

Dong, B., Silverman, R.H., 1997. A bipartite model of 2–5A-dependent RNase L. J. Biol. Chem. 272 (35), 22236–22242.

Han, J.Q., Townsend, H.L., Jha, B.K., Paranjape, J.M., Silverman, R.H., Barton, D.J., 2007. A phylogenetically conserved RNA structure in the poliovirus open reading frame inhibits the antiviral endoribonuclease RNase L. J. Virol. 81 (11), 5561–5572.

Hartmann, R., Justesen, J., Sarkar, S.N., Sen, G.C., Yee, V.C., 2003. Crystal structure of the 2′-specific and double-stranded RNA-activated interferon-induced antiviral protein 2′-5′-oligoadenylate synthetase. Mol. Cell. 12 (5), 1173–1185.

Hovanessian, A.G., Justesen, J., 2007. The human 2′-5′oligoadenylate synthetase family: unique interferon-inducible enzymes catalyzing 2′-5′ instead of 3′-5′ phosphodiester bond formation. Biochimie 89 (6–7), 779–788.

Imai, J., Torrence, P.F., 1981. An efficient chemical synthesis of adenylyl(2′ goes to 5′)adenylyl(2′ goes to 5′)adenosine [(2′-5′)-oligo(A)]. Methods Enzymol. 79 (Pt B), 233–244.

Justesen, J., Ferbus, D., Thang, M.N., 1980. 2′5′ oligoadenylate synthetase, an interferon induced enzyme: direct assay methods for the products, 2′5′ oligoadenylates and 2′5′ co-oligonucleotides. Nucleic Acids Res. 8 (14), 3073–3085.

Kajaste-Rudnitski, A., Mashimo, T., Frenkiel, M.P., Guenet, J.L., Lucas, M., Despres, P., 2006. The 2′,5′-oligoadenylate synthetase 1b is a potent inhibitor of West Nile virus replication inside infected cells. J. Biol. Chem. 281 (8), 4624–4637.

Kim, E.E., Wyckoff, H.W., 1991. Reaction mechanism of alkaline phosphatase based on crystal structures. Two-metal ion catalysis. J. Mol. Biol. 218 (2), 449–464.

Kitade, Y., Nakata, Y., Hirota, K., Maki, Y., Pabuccuoglu, A., Torrence, P.F., 1991. 8-Methyladenosine-substituted analogues of 2–5A: synthesis and their biological activities. Nucleic Acids Res. 19 (15), 4103–4108.

Kodym, R., Kodym, E., Story, M.D., 2009. 2′-5′-Oligoadenylate synthetase is activated by a specific RNA sequence motif. Biochem. Biophys. Res. Commun. 388 (2), 317–322.

Lesiak, K., Imai, J., Floyd-Smith, G., Torrence, P.F., 1983. Biological activities of phosphodiester linkage isomers of 2–5A. J. Biol. Chem. 258 (21), 13082–13088.

Malathi, K., Dong, B., Gale Jr., M., Silverman, R.H., 2007. Small self-RNA generated by RNase L amplifies antiviral innate immunity. Nature 448 (7155), 816–819.

Marie, I., Blanco, J., Rebouillat, D., Hovanessian, A.G., 1997. 69-kDa and 100-kDa isoforms of interferon-induced (2′–5′) oligoadenylate synthetase exhibit differential catalytic parameters. Eur. J. Biochem. 248 (2), 558–566.

Min, J.Y., Krug, R.M., 2006. The primary function of RNA binding by the influenza A virus NS1 protein in infected cells: Inhibiting the 2′-5′ oligo (A) synthetase/RNase L pathway. Proc. Natl. Acad. Sci. U. S. A. 103 (18), 7100–7105.

Nakanishi, M., Tanaka, N., Mizutani, Y., Mochizuki, M., Ueno, Y., Nakamura, K.T., Kitade, Y., 2005. Functional characterization of 2′,5′-linked oligoadenylate binding determinant of human RNase L. J. Biol. Chem. 280 (50), 41694–41699.

Rebouillat, D., Hovanessian, A.G., 1999. The human 2′,5′-oligoadenylate synthetase family: interferon-induced proteins with unique enzymatic properties. J. Interferon Cytokine Res. 19 (4), 295–308.

Rebouillat, D., Hovnanian, A., Marie, I., Hovanessian, A.G., 1999. The 100-kDa 2′,5′-oligoadenylate synthetase catalyzing preferentially the synthesis of dimeric pppA2′p5′A molecules is composed of three homologous domains. J. Biol. Chem. 274 (3), 1557–1565.

Roberts, W.K., Hovanessian, A., Brown, R.E., Clemens, M.J., Kerr, I.M., 1976. Interferon-mediated protein kinase and low-molecular-weight inhibitor of protein synthesis. Nature 264 (5585), 477–480.

Rusch, L., Dong, B., Silverman, R.H., 2001. Monitoring activation of ribonuclease L by 2′,5′-oligoadenylates using purified recombinant enzyme and intact malignant glioma cells. Methods Enzymol. 342, 10–20.

Rushizky, G.W., Sober, H.A., 1963. Studies on the specificity of ribonuclease T2. J. Biol. Chem. 238, 371–376.

Sarkar, S.N., Sen, G.C., 1998. Production, purification, and characterization of recombinant 2′, 5′-oligoadenylate synthetases. Methods 15 (3), 233–242.

Sawicki, D.L., Silverman, R.H., Williams, B.R., Sawicki, S.G., 2003. Alphavirus minus-strand synthesis and persistence in mouse embryo fibroblasts derived from mice lacking RNase L and protein kinase R. J. Virol. 77 (3), 1801–1811.

Sen, G.C., 2001. Viruses and interferons. Annu. Rev. Microbiol. 55, 255–281.

Servant, M.J., Grandvaux, N., Hiscott, J., 2002. Multiple signaling pathways leading to the activation of interferon regulatory factor 3. Biochem. Pharmacol. 64 (5–6), 985–992.

Shuman, S., 1990. Catalytic activity of vaccinia mRNA capping enzyme subunits coexpressed in *Escherichia coli*. J. Biol. Chem. 265 (20), 11960–11966.

Silverman, R.H., 2007a. A scientific journey through the 2–5A/RNase L system. Cytokine Growth Factor Rev. 18 (5–6), 381–388.

Silverman, R.H., 2007b. Viral encounters with 2′,5′-oligoadenylate synthetase and RNase L during the interferon antiviral response. J. Virol. 81 (23), 12720–12729.

Smith, J.A., Schmechel, S.C., Williams, B.R., Silverman, R.H., Schiff, L.A., 2005. Involvement of the interferon-regulated antiviral proteins PKR and RNase L in reovirus-induced shutoff of cellular translation. J. Virol. 79 (4), 2240–2250.

Tanaka, N., Nakanishi, M., Kusakabe, Y., Goto, Y., Kitade, Y., Nakamura, K.T., 2004. Structural basis for recognition of 2′,5′-linked oligoadenylates by human ribonuclease L. Embo J. 23 (20), 3929–3938.

Thakur, C.S., Jha, B.K., Dong, B., Das Gupta, J., Silverman, K.M., Mao, H., Sawai, H., Nakamura, A.O., Banerjee, A.K., Gudkov, A., Silverman, R.H., 2007. Small-molecule

activators of RNase L with broad-spectrum antiviral activity. Proc. Natl. Acad. Sci. U. S. A. 104 (23), 9585–9590.
Xiang, Y., Condit, R.C., Vijaysri, S., Jacobs, B., Williams, B.R., Silverman, R.H., 2002. Blockade of interferon induction and action by the E3L double-stranded RNA binding proteins of vaccinia virus. J. Virol. 76 (10), 5251–5259.
Xiang, Y., Wang, Z., Murakami, J., Plummer, S., Klein, E.A., Carpten, J.D., Trent, J.M., Isaacs, W.B., Casey, G., Silverman, R.H., 2003. Effects of RNase L mutations associated with prostate cancer on apoptosis induced by 2′,5′-oligoadenylates. Cancer Res. 63 (20), 6795–6801.
Xiao, W., Player, M.R., Li, G., Zhang, W., Lesiak, K., Torrence, P.F., 1996. Synthesis and characterization of composite nucleic acids containing 2′, 5′-oligoriboadenylate linked to antisense DNA. Antisense Nucleic Acid Drug Dev. 6 (4), 247–258.